Drug Development and Industrial Pharmacy, 27(1), 31–38 (2001)

RESEARCH PAPER

Characterizing Colloidal Structures of Pseudoternary Phase Diagrams Formed by Oil/Water/Amphiphile Systems

Raid G. Alany,* Ian G. Tucker, Nigel M. Davies, and Thomas Rades

School of Pharmacy, University of Otago, P.O. Box 913, Dunedin 9001, New Zealand

ABSTRACT

Two pseudoternary phase diagrams were constructed using ethyl oleate, water, and a surfactant blend containing poly (oxyethylene 20) sorbitan monooleate and sorbitan monolaurate with or without the cosurfactant 1-butanol. Two colloidal regions were identified in the cosurfactant-free phase diagram; a microemulsion (ME) and a region containing lamellar liquid crystals (LC). The addition of 1-butanol increased the area in which systems formed microemulsions and eliminated the formation of any liquid crystalline phases. Samples that form the colloidal regions of both systems were investigated by freeze-fracture transmission electron microscopy and by viscosity and conductivity measurements. The three techniques were compared and evaluated as characterisation tools for such colloidal systems and also to identify transitions between the colloidal systems formed. A droplet ME was present at a low water volume fraction (ϕ_w) in both systems ($\phi_w < 0.15$) as revealed by electron microscopy. At higher ϕ_w values, LC structures were observed in micrographs of samples taken from the cosurfactant-free system while the structure of samples from the cosurfactant-containing system was that of a bicontinuous ME. The viscosity of both systems increased with increasing ϕ_w to 0.15 and flow was Newtonian. However, formation of LC in the cosurfactant-free system resulted in a dramatic increase in viscosity that was dependent on ϕ_w and a change to pseudoplastic flow. In contrast, the viscosity of the bicontinuous ME was independent of ϕ_w. Three different methods

*To whom correspondence should be addressed. Fax 64 3 479 7034. Email: raidalany@hotmail.com

were used to estimate the percolation threshold from the conductivity data for the cosurfactant-containing system. The use of nonlinear curve fitting was found to be most useful yielding a value close to 0.15 for the ϕ_w.

KEY WORDS: Conductivity; Electron microscopy; Microemulsion; Percolation threshold; Viscosity.

INTRODUCTION

Microemulsions (MEs) are optically isotropic, thermodynamically stable, spontaneously forming colloidal systems that form when appropriate combinations of oil, water, and surfactant/cosurfactant are mixed. At low concentrations of oil, the microstructure is often considered to be that of oil-swollen micelles in a continuous aqueous matrix. Conversely, at low water concentrations, inverted water-swollen micelles are considered to be present in an oil continuous matrix. Both can be described as droplet MEs (1). In some systems, a continuous transition from a water-in-oil (w/o) to an oil-in-water (o/w) droplet ME on increasing water volume fraction occurs through a bicontinuous region. In this region, swollen micelles and swollen reverse micelles are rapidly fluctuating and lacking long-range order, the interface separating oil from water is proposed to behave as a surface of constant mean curvature, which nowhere closes on it self. In other systems, the single-phase, oil-rich, and water-rich regions are disjointed and are separated by a composition zone in which liquid crystalline structures (LCs) and coarse dispersions are present (2).

MEs and LCs have unique properties, which may render them useful in drug delivery. MEs are easy to prepare, clear, and stable and have low viscosity. Depending on the type of ME, they can effectively solubilize either oil-soluble, water-soluble, or amphiphilic materials because of their extensive oily, aqueous and, interfacial domains. Their enormous interfacial areas and ultralow interfacial tensions may also be beneficial in promoting drug transport (3). LCs, on the other hand, have a higher viscosity and have found use in stabilizing many pharmaceutical dosage forms including simple and multiple emulsions, creams, and gels (4).

To exploit these colloidal systems in drug delivery, it is important that scientists involved in formulation and development are able to readily identify the type of system formed by a particular oil/water/amphiphile combination. The behavior of oil/water/amphiphile systems is usually investigated by the construction of a ternary or a pseudoternary phase diagram for the respective components and characterizing the systems formed by the various combinations.

The aim of this investigation was to evaluate and compare three commonly available laboratory techniques to identify the various colloidal structures, which are often present in such phase diagrams and the transitions between these structures. Two different phase diagrams were constructed. A pseudoternary system having a droplet ME region and a region containing LC was prepared from the two non-ionic surfactants, sorbitan monolaurate and poly (oxyethylene 20) sorbitan mono-oleate, with ethyl oleate as the oil component and water. A pseudoternary system having both a droplet and a bicontinuos ME was prepared by inclusion of 1-butanol to perturb the formation of the LC phase (5).

MATERIALS AND METHODS

Materials

Ethyl oleate was used as the oil component (Crodamol EO™). Sorbitan monolaurate (Crill 1™) and polyoxyethylene 20 sorbitan mono-oleate (Crillet 4 super™) were used as surfactants. All three compounds were provided by Croda Oleo-chemicals (Auckland, New Zealand). 1-Butanol used as cosurfactant, and sodium chloride used for conductivity measurements were obtained from BDH Chemicals Ltd (Poole, UK). All chemicals were used without further purification. De-ionized water (specific conductance ≤ 0.1 S·cm^{-1} at room temperature) was used in the preparation of all samples in the phase diagrams.

Methods

Construction of Pseudoternary Phase Diagrams

Mixtures of ethyl oleate, surfactants, or a surfactants/cosurfactant blend, and water of various weight ratios were prepared and left overnight at room temperature to equilibrate. A 6:4 weight ratio of poly (oxyethylene 20) sorbitan mono-oleate and sorbitan monolaurate was used as the surfactant blend. The blend was chosen according to the combination that solubilized the greatest amount of water on titration when various blends of the two surfactants were mixed with ethyl oleate at a mass ratio of 1:1 (6). The same approach was used to determine

the surfactant blend:cosurfactant ratio of 7:3 used in this investigation.

Visual observation and phase-contrast and polarizing light microscopy (Nikon Optiphot PFX microscope, Tokyo, Japan) were used to identify combinations forming MEs, LC-containing regions, and coarse emulsions. Clear, isotropic one-phase systems were classified as MEs, whereas opaque systems showing birefringence with typical oily streaks, maltese crosses, or fan-shaped textures when viewed by cross-polarized light microscopy were classified as systems containing lamellar LCs. Systems identified as consisting of two-phases when viewed by phase-contrast microscopy and showing no birefringence under a cross-polarizer were classified as coarse emulsions. The pseudoternary phase diagrams for both the cosurfactant-free and cosurfactant-containing systems are shown in Figure 1(a) and (b), respectively.

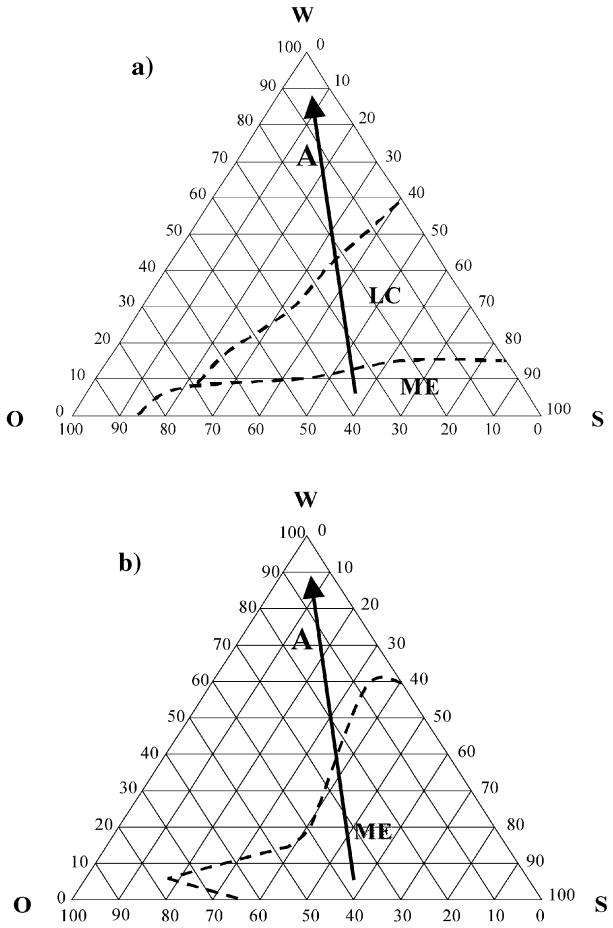

Figure 1. Pseudoternary phase diagrams: (a) cosurfactant-free system, (b) cosurfactant-containing system. Both show the sampling path along the arrow A. W indicates 100% water; O, 100% ethyl oleate; S, 100% surfactant blend, or surfactant blend: 1-butanol (7:3) ME, microemulsion region; LC, region containing lamellar liquid crystals.

Characterization of Colloidal Systems

Systems lying on the sampling path marked by the arrow A on the phase diagram spanning form the 40:60 oil:amphiphile system to the water apex were used for characterization. Samples were prepared by progressively adding water to the oil:amphiphile blends at increments of 1 to 5% w/w. After equilibration, the samples were characterized by freeze-fracture transmission electron microscopy (FF-TEM) and measurements of viscosity and electrical conductivity.

For FF-TEM, two copper support disks and a TEM grid (400 mesh) were used. The TEM grid was immersed into the microemulsion and then sandwiched between two flat copper disks. The sandwich was then snap-frozen by immersion in liquid propane (-180°C) and then loaded into a double-replica device immersed in liquid nitrogen (-196°C). For fracturing, the double-replica device was mounted on the rotary sample stage of a Balzers BAF 300 freeze etch device (Balzers, Liechtenstein) cooled to -110°C. Fracturing was carried out at a vacuum of 6.5×10^{-4} Pa. The fractured surfaces were shadowed with platinum (45°) and then immediately with carbon (90°). The replicas were then washed in chloroform, methanol, and finally distilled water. The replicas were mounted onto copper grids and viewed with a Philips 410 LS transmission electron microscope (Philips, Eindhoven, The Netherlands) operating at an accelerating voltage of 80 kV.

Viscosity of the systems was measured using a Brookfield DVIII viscometer (Brookfield Engineering Laboratories Inc., Stoughton, MA) fitted with either a CP-42 or CP-52 cone spindle. Electrical conductivity was measured using a Riac CM/100 conductivity meter with a YSI 3418 electrode (Yellow Springs Instruments Inc., Yellow Springs, OH). The cell constant for the electrode was 0.11 cm^{-1}. For conductivity measurements, a 1μM solution of sodium chloride was used as the aqueous phase and readings were taken after the value had remained constant for at least 5 min. Incorporation of 1μM sodium chloride did not effect the phase behavior of either systems. All viscosity and conductivity measurements were carried out in triplicate at 25°C.

RESULTS AND DISCUSSION

For the surfactant blend/oil/water system, samples along the sampling path A (Fig. 1) remained optically

clear and isotropic up to an added water-volume fraction (ϕ_w) of 0.15. Thereafter, up to a ϕ_w of 0.45, a second, opaque phase separated after equilibration exhibiting birefringence when viewed under cross-polarized light having textures typical of lamellar LCs. The volume of the system occupied by the LC phase was dependent on ϕ_w and was present in equilibrium with either an oily or an aqueous phase, again dependent on the ϕ_w added to the system. Addition of >0.45 ϕ_w to the 40:60 oil:surfactant blend system resulted in isotropic two-phase systems having an aqueous continuous phase. For the cosurfactant-containing system, samples remained clear and isotropic up to a ϕ_w of 0.37 beyond which isotropic two-phase systems were again observed.

The increased tendency of the pseudoternary system to form MEs on addition of 1-butanol has been reported (5). Alcohols are often used as cosurfactants to promote the formation of MEs in combination with a surfactant or surfactant blend. Cosurfactants act by further reducing the interfacial tension between the oil and water phases, by increasing the flexibility of the interfacial film, and by interacting with either the head-group or the tail-group region of the surfactant, thereby influencing film curvature (7). Short-chain alcohols, such as 1-butanol, are believed to interact with the head region of the surfactant leading to a more positive curvature of the surfactant monolayer, which should hinder bending around water-swollen reverse micelles (8).

Electron micrographs (EMs) of freeze-fractured samples of representative systems formed along the sampling path marked by the arrow A in the two phase diagrams spanning from the 40:60 oil:amphiphile pseudobinary system to the water apex are shown in Figure 2. The EMs depicted in Figure 2(a) and (e) are representative of the structures observed in grids prepared from the pseudobinary systems formed when the oil is mixed with either the surfactant blend (poly (oxyethylene 20) sorbitan monooleate and sorbitan monolaurate at a weight ratio of 6:4) or the surfactant blend/1-butanol mixture (at a weight ratio of 7:3). Both systems show a uniform appearance resulting from the deposition of the shadowing material on the oil fracture face with the absence of any obvious structures. The EMs depicted in Figure 2(b) and (f) are representative of samples of the cosurfactant-free system after addition of $0.05\phi_w$ or of the cosurfactant-containing system after addition of $0.075\phi_w$. In both cases, isolated globular structures embedded in a matrix having a similar appearance to the water-free pseudobinary system are observed. Similar structures can be observed but with increased frequency in the EM of the cosurfactant-free system having a ϕ_w of 0.125 [Fig. 2(c)]. The globular structures in all cases have

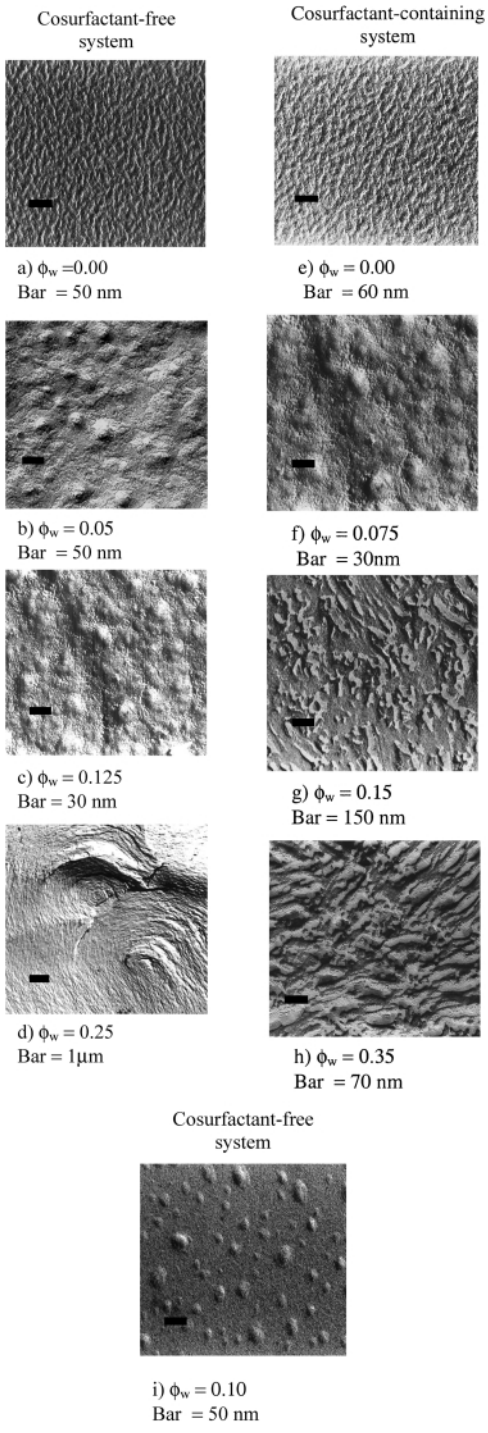

Figure 2. Freeze-fracture transmission electron micrographs of the cosurfactant-free (a–d) and 1-butanol (e–h) systems. Magnification and water volume fraction (ϕ_w) is indicated on each micrograph. Micrograph (i) represents an ice contamination artifact formed during the sample freezing precess and is included for comparison.

a diameter <100 nm. This is preliminary evidence for the existence of a droplet ME where swollen reverse micelles form in an oil-rich matrix on the addition of water to the pseudobinary system, with their number increasing with ϕ_w (9).

Globular structures can also result from ice contamination. Figure 2(i) is included for comparison and shows ice droplets decorating the surface of the replica. Ice decoration is a frequently encountered artifact in FF-TEM. The ice particles appear aligned in a single direction at the surface of the replica rather than embedded in the background. Their appearance is clearly different from the structures visualised in Figure 2(b) and (c).

Addition of $>0.15\phi_w$ to the cosurfactant-free system resulted in the formation of a phase containing lamellar LCs as observed by polarized light microscopy. Figure 2(d) is a representative EM of a freeze-fractured sample after addition of $0.25\phi_w$ to the pseudobinary cosurfactant-free system. The micrograph shows the characteristic multilayer structure of a lamellar mesophase with typical nonplanar defect structures (10). Such structures were observed in samples up to a ϕ_w of 0.45 in the cosurfactant-free system.

The effect of increasing the ϕ_w beyond 0.15 in the system containing 1-butanol is shown in Figure 2(g) and (h). These samples were clear and isotropic and thus classified as microemulsions. However, it can be seen from the EMs that the structure is different from that noted for a droplet microemulsion observed at a ϕ_w of 0.075. Oil domains (seen as the darker areas having the characteristic decorative appearance of the shadow material as noted in the pseudobinary systems) and water domains are intertwined and the interface has a fluctuating curvature. At a ϕ_w of 0.15, the larger oil continuous domains dominate [Fig. 2(g)]. However, the density of the water domains is seen to increase with increasing ϕ_w [Fig. 2(h)]. No structures characteristic of lamellar LCs were observed in any of the samples. Such observations are characteristic of a bicontinuous ME (9). Thus, addition of the short-chained alcohol 1-butanol to the pseudoternary system has perturbed the formation of an LC region in the phase diagram, favoring instead the formation of a bicontinuous ME.

Figure 3 illustrates how the viscosity of the two systems is affected by ϕ_w. Two regions can be identified in the profiles of both systems (below and above ϕ_w of 0.15). At ϕ_w of less than approximately 0.15 all systems were fluid and exhibited Newtonian flow, and the viscosity was found to increase with increasing ϕ_w. Inclusion of the cosurfactant, however, yielded systems having a lower viscosity compared with the corresponding

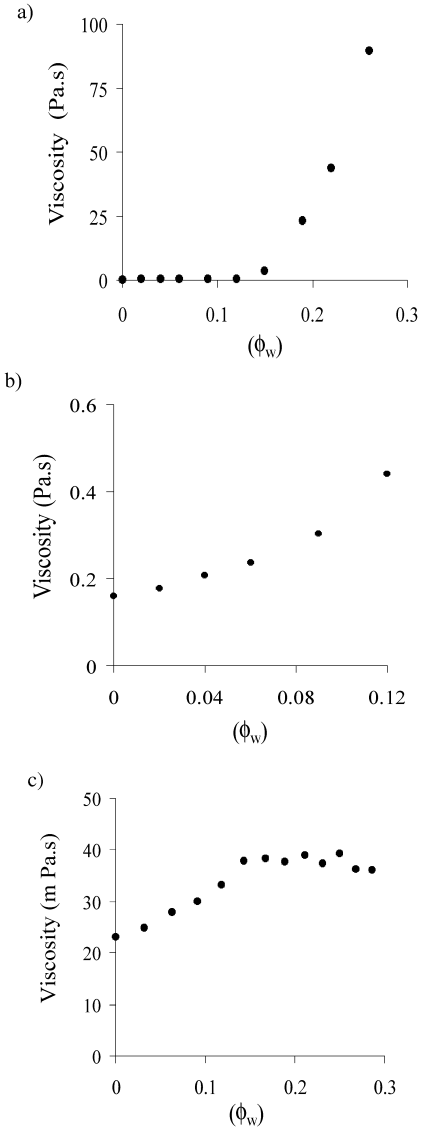

Figure 3. Effect of ϕ_w on viscosity for (a) cosurfactant-free system (ME and LC regions), (b) cosurfactant-free system (ME region, expanded scale, (c) cosurfactant-containing system.

cosurfactant-free systems. At ϕ_w of approximately 0.15, the flow of cosurfactant-free systems changed from Newtonian to non-Newtonian (pseudoplastic) with increasing ϕ_w. The change in type of rheological flow coincides with the emergence of lamellar LCs as identified by light and electron microscopy. FF-TEM demonstrated the existence of nonplanar defect structures in the lamellar LC phase, which on increasing shear-rate may align in the direction of flow resulting in pseudoplastic behavior. The apparent viscosity of these systems was calculated according to the

following modified viscosity equation (11):

$$\log D = \log 1/\eta + \mathrm{n} \log \tau \quad (1)$$

where D is the shear rate, τ is the shear stress, η is the apparent viscosity, and n is the index of deviation from Newtonian flow behavior. The apparent viscosity of the systems further increased with ϕ_w up to 0.25, corresponding to the increased phase volume occupied by the LC phase.

For the cosurfactant-containing systems, the flow remained Newtonian up to a ϕ_w of 0.37, coinciding with the phase boundary between the ME region and the coarse oil in water emulsion. Above a ϕ_w of 0.15, the viscosity of systems containing 1-butanol was independent of ϕ_w and the systems remained more fluid than the corresponding systems, which did not contain the cosurfactant, i.e., LC-containing systems. FF-TEM showed the structure of cosurfactant-containing systems having a ϕ_w of >0.15 and <0.37 to be that of a bicontinuous ME. Bicontinuous MEs are dynamic structures with a continous fluctuation occurring between the bicontinuous structure, swollen reverse micelles, and swollen micelles (2). Despite being topologically ordered as a result of the surfactant's tendency to form sheets between the oil-rich and water-rich domains, they are geometrically disordered (12,13). In this regard, they may be distinguished from the geometrically ordered LC structures, which have an associated much higher viscosity.

Measurement of electrical conductivity can also be used to monitor structural changes in MEs (14). For both the cosurfactant-free and the 1-butanol systems, the specific conductance (κ) increased with ϕ_w. However, in all cases, κ was greater for the 1-butanol system than for the corresponding cosurfactant-free system [Fig. 4(a)]. Figure 4(b) (expanded scale) shows the changes in κ for the cosurfactant-free system below a ϕ_w of 0.2. An initial increase in κ that reaches a maximum at $\phi_w \approx 0.04$ is observed, which is followed by a decrease to $\phi_w \approx 0.13$, beyond which a further increase in κ is noted with increasing ϕ_w. The increase of κ up to $\phi_w \approx 0.04$ may be a result of the progressive increase in the hydration of the ethylene oxide moieties of the head group of monomeric poly (oxyethylene 20) sorbitan mono-oleate surfactant, rendering a better conducting entity that possibly exists in rapid equilibrium with reverse micelles. The decrease in κ noted between ϕ_w of 0.04 and 0.13 may be a result of surfactant aggregation forming swollen reverse micelles, i.e., replacement of hydrated monomeric surfactant molecules with water-cored swollen reverse micelles having a higher surfactant aggregation number than do reverse micelles. The increase in κ beyond the ϕ_w minimum of 0.13 is the result of the reorganization of reverse swollen micelles forming structured liquid crystals. The increase in κ beyond ϕ_w of 0.13 coincides with the detection of birefringence when the samples were viewed by polarizing light microscopy.

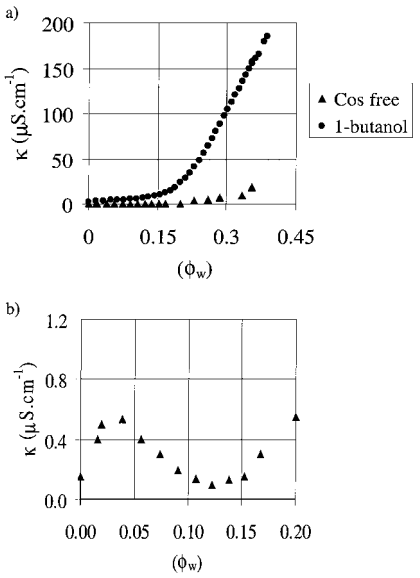

Figure 4. Specific conductance (κ) as a function of the water volume fraction (ϕ_w) for cosurfactant-free and cosurfactant-containing (1-butanol) systems. (b) Specific conductance (κ) as a function of the water volume fraction (ϕ_w) for the cosurfactant-free system (expanded scale).

No local maximum in κ was noted with increased ϕ_w for the 1-butanol system. This suggests that no minimum ϕ_w is required before swollen reverse micelles begin to form. The ethylene oxide moieties of the head group of monomeric poly (oxyethylene 20) sorbitan mono-oleate surfactant may already be associated with the short-chained alcohol in the absence of water. Addition of water may then immediately encourage the formation of water-swollen reverse micelles.

At a ϕ_w of <0.15, κ of both systems is low. At this stage the structure of the systems is that of a droplet ME in which the continuous phase is the oil. The conductive entities, being the water droplets, are isolated from each other accounting for the low κ. For the 1-butanol system, when ϕ_w reaches and exceeds a critical value known as the percolation threshold (ϕ_p), droplets begin to contact each other, forming clusters with many conductive paths so κ of the system then increases dramatically [Fig. 4(a)]. Thus, the inflection on the plot of κ against ϕ_w is representative of ϕ_p and corresponds to the transformation from a droplet to a bicontinuous ME. Providing that there is a distinct inflection in the curve, an estimate of ϕ_p can be obtained by plotting the first derivative of $\kappa(\mathrm{d}(\log_{10}\kappa)/\mathrm{d}\phi_w)$ against ϕ_w

and locating the maximum (15). The accuracy of this approach in predicting ϕ_p, however, depends on the number of data points collected.

The profile of the plot of κ against ϕ_w can also be interpreted using the concept of percolative conduction phenomena in inhomogeneous media and effective medium theory (16). The usefulness of these two concepts in the understanding of the conductive behavior of ME systems has previously been reported (17). Accordingly, in the vicinity of the percolation threshold ϕ_p, the dependency of κ on ϕ_w can be described by the following relationships:

$$\kappa \approx (\phi_p - \phi_w)^{-s} \qquad \text{when } \phi_p > \phi_w \tag{2}$$

and

$$\kappa \approx (\phi_w - \phi_p)^{t} \qquad \text{when } \phi_w > \phi_p \tag{3}$$

The values of the constants, s (0.5-1.2) and t (1.2-2.1) depend on the dimensionality (i.e., number of variables) of the system. Several modifications of the these equations have been reported in the literature (18–20). The percolation threshold for a system can, therefore, also be estimated by randomly selecting values for t within the specified range and plotting ϕ_w against $\kappa^{1/t}$ (at $\phi_w > \phi_p$). The value, which yields a linear relationship, is considered the appropriate model and can be used to estimate ϕ_p (17). A drawback to this approach, however, is that the values of t have to be arbitrarily selected and changed until a value yielding a linear relationship is found. Thus, multiple analyses are required and only the data points $>\phi_p$ are used.

Alternatively, the data can be nonlinearly modeled using Eq. 2 and Eq. 3 to describe the complete dataset, and s, t, and ϕ_p estimated from the data. Consequently, the number of data points collected becomes less critical, in contrast to the first-derivative approach. In this study, we compared the applicability of the nonlinear curve fitting using the computer software Minim version 3.0 (21), with the two previously published methods of estimating ϕ_p, namely the first derivative approach (15) and the power-scaling approach (17). Figure 5(a) shows the first derivative plot for the 1-butanol system. From this plot, ϕ_p is estimated at 0.184. The most linear relationship between κ and ϕ_w (when $\phi_w > \phi_p$) for the same system, was noted when κ was raised to 1/1.2 yielding a r^2 of 0.99 [Fig. 5(b)]. Extrapolation of the data gave an estimate of 0.166 for ϕ_p. Nonlinear curve fitting using the entire dataset estimated ϕ_p to be 0.155 ± 0.0023 with a correlation coefficient of 0.999. The values of s and t were estimated at 0.166 and 1.28, respectively. The deviation of s from the literature range (0.5 to 1.2) has been reported previously by other investigators (15,17) and was attributed to droplet motion as opposed to static systems for which the above-mentioned

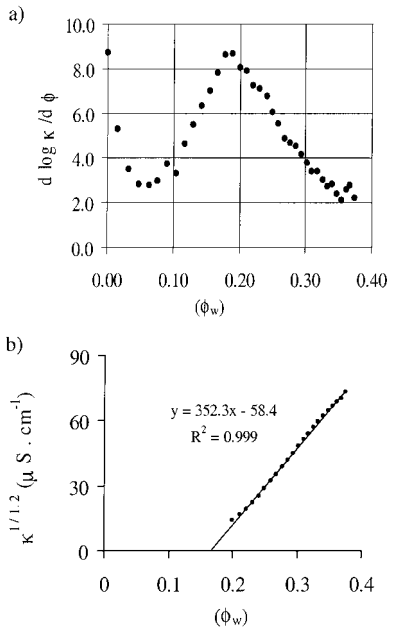

Figure 5. Plot of $d \log \kappa / d\phi$ versus ϕ_w used for estimating percolation threshold (ϕ_p) according to the first derivative approach. (b) Plot of $\kappa^{1/1.2}$ versus ϕ_w used for calculating the percolation threshold (ϕ_p) using the power scaling approach.

range applies. It was found that nonlinear curve fitting also required multiple analysis because it was necessary to determine which data were above and below ϕ_p to obtain the best correlation. Once the data had been appropriately classified, it was found that the predicted ϕ_p was independent of the initial estimate. However, despite requiring multiple analysis, nonlinear regression was considered an improved method of estimating ϕ_p because it did not require data manipulation and it used all the data collected. The value of ϕ_p predicted by nonlinear regression was close to that predicted by the power-scaling approach but was significantly lower than that predicted by the first-derivative approach. The value predicted by power-scaling and nonlinear regression, however, was more in agreement with the point of inflection noted in the plot of viscosity against ϕ_w [Fig. 3(c)] than that predicted by the first-derivative approach, and all corresponded with the area in which structural changes were observed by FF-TEM.

CONCLUSION

The microstructure of colloidal systems frequently encountered in pseudoternary systems of oil, water, and amphiphiles, namely droplet MEs, bicontinuous MEs, and LC and the transitions between these structures can be

identified and studied to an extent often sufficient in formulation development by a combination of polarized and phase-contrast light-microscopy, FF-TEM, and measurements of viscosity and conductivity. Microscopy is invaluable in determining the type of colloidal dispersion present, but FF-TEM requires more elaborate sample preparation than does measurements of viscosity and conductivity and also requires discrimination between artifacts and what may be considered true structures. Rheological evaluation readily distinguishes between systems that change from droplet MEs to bicontinuous MEs and those that change to systems containing LCs as the viscosity of systems containing the more structured and rigid LC is higher and demonstrate pseudoplastic flow behavior. Electrical conductivity measurements are not only useful in determining the nature of the continuous phase, but also the magnitude of change enable estimation of the percolation threshold of such systems. Knowledge of the percolation threshold of such systems may have important implications in drug delivery.

ACKNOWLEDGMENT

The authors wish to thank Mark Gould of the South Campus Electron Microscope unit, University of Otago, for his assistance in sample preparation for the FF-TEM.

REFERENCES

1. Attwood, D. Microemulsions. In *Colloidal Drug Delivery Systems*; Kreuter, J., Ed.; Marcel Dekker Inc.: New York, 1994; 31–71.
2. Bourrel, M.; Schechter, R.S. The R ratio. In *Microemulsions and Related Systems*; Bourrel, M., Schechter, R.S., Eds.; Marcel Dekker: New York, 1988; 1–30.
3. Lawrence, M.J. Surfactant Systems: Microemulsions and Vesicles as Vehicles for Drug Delivery. Eur. J. Drug Metab. Pharmacokinet. **1994**, *3*, 257–269.
4. Tyle, P. Liquid Crystals and Their Application in Drug Delivery. In *Controlled Release of Drugs: Polymers and Aggregate Systems*; Rosoff, M., Ed.; VCH publishers Inc.: New York, 1989; 125–161.
5. Alany, R.G.; Rades, T.; Agatonovic-Kustrin, S.; Davies, N.M.; Tucker, I.G. Effects of Alcohols and Diols on the Phase Behaviour of Quaternary Systems. Int. J. Pharm. **2000**, *196* (2), 141–145.
6. Alany, R.G.; Agatonovic-Kustrin, S.; Rades, T.; Tucker, I.G. Use of Artificial Neural Networks to Predict Quaternary Phase Systems from Limited Experimental Data. J. Pharm. Biomed. Analysis. **1999**, *19*, 443–452.
7. De Gennes, P.G.; Taupin, C. Microemulsions and Flexibility of Oil/Water Interfaces. J. Phys. Chem. **1982**, *86*, 2294–2304.
8. Fletcher, D.I.; Parrott, D. Protein Partitioning between Microemulsion Phases and Conjugate Aqueous Phases. In *Structure and Reactivity in Reverse Micelles*; Pileni, M.P., Ed.; Elsevier: New York, **1989**, 303–322.
9. Jahn, W.; Strey, R. Microstructure of Microemulsions by Freeze Fracture Electron Microscopy. J. Phys. Chem., **1988**, *92*, 2294–2301.
10. Rades, T.; Müller-Goymann, C.C. Electron and Light Microscopical Investigations of the Defect Structures in Mesophases of Pharmaceutical Substances. Colloid Polym. Sci. **1997**, *275*, 1169–1178.
11. Kabre, S.P.; DeKay, H.G.; Banker, G.S. Rheology and Suspension Activity of Pseudoplastic Polymers I. J. Pharm. Sci. **1964**, *53*, 492–495.
12. Kaler, E.W.; Bennett, K.E.; Davis, H.T.; Scriven, L.V. Toward Understanding Microemulsion Microstructure: A Small-Angle X-Ray Scattering Study. J. Phys. Chem. **1983a**, *79*, 5673–5684.
13. Kaler, E.W.; Bennett, K.E.; Davis, H.T.; Scriven, L.V. Toward Understanding Microemulsion Microstructure. II. J. Phys. Chem. **1983b**, *79*, 5685–5692.
14. Kahlweit, M.; Strey, R.; Hasse, D.; Kunieda, H.; Schmeling, T.; Faulhaber, B.; Borkovec, M.; Eicke, H.-F.; Busse, G.; Eggers, F.: Funck, T.H.; Richmann, H.; Magid, L.; Söderman, O.; Stilbs, P.; Winkler, J.; Dittrich, A.; Jahn, W. How to Study Microemulsions. J. Colloid Interface Sci. **1987**, *118*, 436–453.
15. Mehta, S.K.; Bala, K. Volumetric and Transport Properties in Microemulsions and the Point of View of Percolation Theory. Phys. Rev. E. **1995**, *51*, 5732–5737.
16. Kirkpatrick, S. Classical Transport in Disordered Media: Scaling and Effective Medium Theories. Phys. Rev. Lett. **1971**, *27*, 1722–1725.
17. Laguës, M.; Sauterey, C. Percolation Transition in Water in Oil Microemulsions. Electrical Conductivity Measurements. J. Phys. Chem. **1980**, *84*, 3503–3508.
18. Fang, J.; Venable, R.L. Conductivity Study of the Microemulsion System Sodium Dodecyl Sulfate-Hexylamine-Heptane-Water. J. Colloid Interface Sci. **1987**, *116*, 269–277.
19. Gu, G.; Wang, W.; Yan, H. Electric Percolation of Water-in-Oil Microemulsions: The Application of Effective Medium Theory to System Sodium Dodecylbenzenesulfonate (DDBS)/n-Pentanol/n-Heptane/Water. J. Colloid Interface Sci. **1996**, *178*, 358–360.
20. Ray, S.; Paul, S.; Moulik, S.P. Physicochemical Studies on Microemulsions, V. Additive Effects on the Performance of Scaling Equations and Activation Energy for Percolation of Conductance of Water/AOT/Heptane Microemulsion. J. Colloid Interface Sci. **1996**, *183*, 6–12.
21. Purves, R.D. Anomalous Parameter Estimates in the One Compartment Model with First Order Absorption. J. Pharm. Pharmacol. **1993**, *45*, 934–936.